An Approach for Chaos Synchronization Based on Non-Continuous "Excursion-Orbit" Coupling

Shui-Sheng Qiu[†], Chi K. Tse[*], Yufei Zhou[*#], Xiaoan Zhou[‡] and Xinguo Cai[†]

[*]Department of Electronic and Information Engineering, Hong Kong Polytechnic University, Hong Kong, China.
[†]South China University of Technology, Guangzhou, China.
[‡]Shenzhen University, Shenzhen, China.
[#]Anhui University, Anhui, China.

Abstract

In this paper an approach is proposed for synchronizing chaotic systems, taking the viewpoint of a special characterization of chaotic attractors in which spiraling and excursion orbits are identified as the basic constituents. The proposed synchronization method takes advantage of the fact that a chaotic attractor is strongly characterized by excursion orbit segments, and hence synchronization can be achieved by coupling only the excursion orbit segments. Furthermore, a multiplexing scheme can be applied to the drive signals. Since the systems remain uncoupled for most of the time, the bandwidth required for transmitting the drive signal can be very small.

1. Introduction

Chaos synchronization has been studied widely since Pecora and Carroll [1] first demonstrated the possibility of making two chaotic systems operate in synchrony. The potential application of chaos in communications has catalyzed the research for practical and robust synchronization of chaotic systems [2]–[4].

Our purpose in this paper is to propose a method for synchronizing two chaotic systems. The method is based on a special characterization which essentially decomposes a chaotic attractor into two constituent orbits, namely a spiraling orbit and an excursion orbit. Since the excursion orbit strongly characterizes the chaotic attractor in question, it can be effectively used for coupling, giving rise to a non-continuous approach for chaos synchronization. Since coupling is not required for most of the time, only a small bandwidth is needed for transmitting the drive signals.

2. Review of Characterization of Chaotic Attractors

Recently, the chaos producing mechanism has been studied from the viewpoint of *hybrid attractor* which arises from interaction of a *saddle periodic orbit* and a *saddle focus* [6]. This viewpoint is an extension of Shil'nikov's theorem [7],[8], allowing more convenient characterization of chaotic attractors. Essentially, the saddle periodic orbit pushes away nearby trajectories which are then attracted by the saddle focus. As trajectories approach the saddle focus, they are again repelled away and attracted by the saddle periodic orbit. The saddle focus is associated with a manifold on which trajectories "swirls" in a spiral-like motion, whereas the saddle periodic orbit is associated with a manifold on which trajectories make large-amplitude excursion before falling back onto the other manifold where spiral-motion resumes. Thus, the chaotic attractor "glues" together oscillatory spiral motions and large-amplitude excursions, with the spiral motions defining the natural oscillation frequency and the excursions characterizing the random-like motion. In the following we formally summarize this theoretical viewpoint. Details are found in Qiu [6].

We consider the autonomous system:

$$\frac{d\boldsymbol{x}}{dt} = f(\boldsymbol{x}) \quad \text{for } \boldsymbol{x} \in \mathbf{R}^3 \tag{1}$$

where $f : \mathbf{R}^3 \to \mathbf{R}^3$ is p-times differentiable ($p \geq 1$) with continuous derivatives. The equilibrium point $\boldsymbol{x}_e$ is determined by $f(\boldsymbol{x}_e) = 0$. The linearized system of (1) is

$$\frac{d\boldsymbol{x}}{dt} = Df(\boldsymbol{x}_e)\boldsymbol{x} \tag{2}$$

where $Df(\boldsymbol{x}_e)$ is the Jacobian of f evaluated at $\boldsymbol{x}_e$. Suppose γ and $\sigma \pm j\omega_0$ are the eigenvalues of $Df(\boldsymbol{x}_e)$, where γ, σ and ω_0 are real numbers and $\omega_0 \neq 0$. We call $\boldsymbol{x}_e$ a *saddle focus* if

$$\sigma\gamma < 0. \tag{3}$$

This saddle focus is associated with a stable manifold $\boldsymbol{W}^s(\boldsymbol{x}_e)$ and an unstable manifold $\boldsymbol{W}^u(\boldsymbol{x}_e)$. A saddle periodic orbit (SPO), L, also exists (see [6]). Again, associated with it are a stable manifold $\boldsymbol{W}^s(L)$ and an unstable manifold $\boldsymbol{W}^s(L)$, as depicted in Fig. 1. A segment of the trajectory in the manifold is a combination of a spiraling orbit and an excursion orbit. Let the trajectory be denoted by

$$\boldsymbol{x} = \boldsymbol{x}_e + \tilde{\boldsymbol{x}}_d(t) + \tilde{\boldsymbol{x}}_s(t), \tag{4}$$

where $\tilde{\boldsymbol{x}}_d(t)$ and $\tilde{\boldsymbol{x}}_s(t)$ are the excursion and spiraling orbit, respectively. Depending upon the relative magnitudes of $|\tilde{\boldsymbol{x}}_d(t)|$ and $|\tilde{\boldsymbol{x}}_s(t)|$, either excursion or spiraling dominates. Moreover, if excursion dominates in the local stable or unstable manifold in the neighbourhood of an SPO, we call such an SPO a singular SPO (SSPO). In particular we consider a special kind of SSPO whose unstable manifold contains dominated excursion orbit. A saddle focus and an SSPO of this type constitute a *hybrid attractor* if the directions of the manifolds are consistent with

$$\boldsymbol{W}^u(\boldsymbol{x}_e) = \boldsymbol{W}^s(L) \quad \text{and} \quad \boldsymbol{W}^s(\boldsymbol{x}_e) = \boldsymbol{W}^u(L) \tag{5}$$

This work was supported by Hong Kong Research Grants Council under Grant PolyU5131/99E and the Doctoral Education Foundation of China under Grant 00056107.

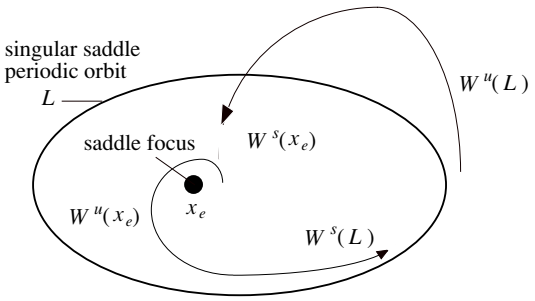

Fig. 1: Hybrid attractor $(\boldsymbol{x}_e, L)$ and circulating flow.

in some subspaces. Thus, there may exist a circulating flow in the neighbourhood of the hybrid attractor. Sufficient conditions are found in Qiu [6] for the existence of chaotic attractors.

From Fig. 1 we see that the chaotic attractor consists of many excursion orbits, and there exists a countable sequence t_n (where $n \in (-\infty, \infty)$) of times at which the nth excursion orbit starts to appear. The dividing point of the nth excursion orbit and its preceding spiraling orbit near L can be found by inspecting ρ_L which is defined by

$$\rho_L = \min\{|\boldsymbol{x} - \boldsymbol{x}_L|\} \quad \text{for } \boldsymbol{x}_L \in L. \tag{6}$$

The dividing point is the point where ρ_L is minimum. Note that $d\rho_L/dt$ has a sharp turning point near the dividing point at which the trajectory moves off rapidly from the basin of L. This property can be used for computation of the dividing point. Likewise, another dividing point, one between the nth excursion orbit and its succeeding spiraling orbit, corresponds to the minimum value of ρ_e, where

$$\rho_e = |\boldsymbol{x} - \boldsymbol{x}_e|. \tag{7}$$

In the next section we will use the aforementioned viewpoint to derive an effective synchronization approach for chaotic systems.

3. Principle of Non-Continuous "Excursion-Orbit" Synchronization

The viewpoint described above essentially looks at a chaotic attractor as being composed of spiraling orbits and excursion orbits. The fundamental frequency of the spiraling orbits is the natural frequency of the associated linearized system, which is non-random. Moreover, excursion orbits come into play "randomly", characterizing the chaotic dynamics of the attractor. Furthermore, the excursion orbits already contain the spiraling motion as small-amplitude oscillations. It can therefore be conceived that two chaotic systems will be synchronized if the randomly varying excursion orbits of one system asymptotically approach those of the other. Hence, we need only to send the excursion orbits as drive signals in order to achieve synchronization.

We consider the error-feedback implementation [9], which can be described in terms of the following drive-response system:

$$\begin{cases} \dot{x}_1 = \alpha(x_2 - x_1 - f(x_1)) \\ \dot{x}_2 = x_1 - x_2 + x_3 \\ \dot{x}_3 = -\beta x_2 \end{cases} \tag{8}$$

and

$$\begin{cases} \dot{y}_1 = \alpha(y_2 - y_1 - f(y_1)) - k_1 k_b (y_1 - x_1) \\ \dot{y}_2 = y_1 - y_2 + y_3 - k_2 k_b (y_2 - x_2) \\ \dot{y}_3 = -\beta y_2 - k_3 k_b (y_3 - x_3) \end{cases} \tag{9}$$

where $f(.)$ defines the characteristic nonlinearity in the Chua's system [10], k_1, k_2, k_3 are the coupling gains, and k_b is equal to 1 when excursion orbit appears, and is 0 when spiraling orbit appears. Suppose the nth excursion orbit appears in the interval $t_n \le t \le t_n + \tau_{nb}$, i.e., the trajectory takes its nth excursion for a duration of τ_{nb} starting at t_n. Note that t_n and $t_n + \tau_{nb}$ correspond to the dividing points discussed in Section 2. Then, we have

$$k_b = \begin{cases} 1 & \text{if } t_n \le t \le t_n + \tau_{nb} \\ 0 & \text{otherwise.} \end{cases} \tag{10}$$

Note that the above method of coupling requires simultaneous transmission of all three drive variables x_1, x_2 and x_3. Moreover, it is possible to derive an alternative simpler coupling scheme, where the three drive variables are transmitted one at a time. In this case, we need only one transmission channel and the drive variables are effectively being multiplexed into one drive signal. The state equations for the response system can be written by replacing (9) by

$$\begin{cases} \dot{y}_1 = \alpha(y_2 - y_1 - f(y_1)) - k_1 k_{b1} (y_1 - x_1) \\ \dot{y}_2 = y_1 - y_2 + y_3 - k_2 k_{b2} (y_2 - x_2) \\ \dot{y}_3 = -\beta y_2 - k_3 k_{b3} (y_3 - x_3) \end{cases} \tag{11}$$

where k_{bi}, for $i = 1, 2$ and 3, are defined by

$$k_{b1} = \begin{cases} 1 & \text{if } t_{n1} \le t < t_{n1} + \frac{\tau_{nb}}{3} \\ 0 & \text{otherwise} \end{cases} \tag{12}$$

$$k_{b2} = \begin{cases} 1 & \text{if } t_{n1} + \frac{\tau_{nb}}{3} \le t < t_{n1} + \frac{2\tau_{nb}}{3} \\ 0 & \text{otherwise} \end{cases} \tag{13}$$

$$k_{b1} = \begin{cases} 1 & \text{if } t_{n1} + \frac{2\tau_{nb}}{3} \le t \le t_{n1} + \tau_{nb} \\ 0 & \text{otherwise} \end{cases} \tag{14}$$

From the foregoing, we see that the synchronization method involves finding the times for the dividing points between spiraling and excursion motions. However, in practice, we may simplify the procedure by an approximate method for locating the times for the dividing points. Specifically, since synchronization does not necessarily requires the exact whole excursion orbit to be sampled, we may use the magnitude of one of the variables to determine the dividing points. For example, as shown in Fig. 2 (a), we can sample the excursion orbit segment when x_1 satisfies

$$m_2 \le x_1 \le m_1 \tag{15}$$

for the case where the excursion goes between the neighborhoods of two saddle foci. Moreover, when the excursion returns to the neighborhood of the same saddle focus, we may use

$$x_1 \ge m \tag{16}$$

for locating the dividing points. See Fig. 2 (b).

4. Example: Synchronization of Chua's Circuits

In this section we apply the proposed synchronization approach to the Chua's circuits. Fig. 3 shows two Chua's circuits forming a drive and response system pair. The state variables are v_{S1}, v_{S2} and i_{s3} for the drive system, and v_{R1}, v_{R2} and i_{R3} for the response

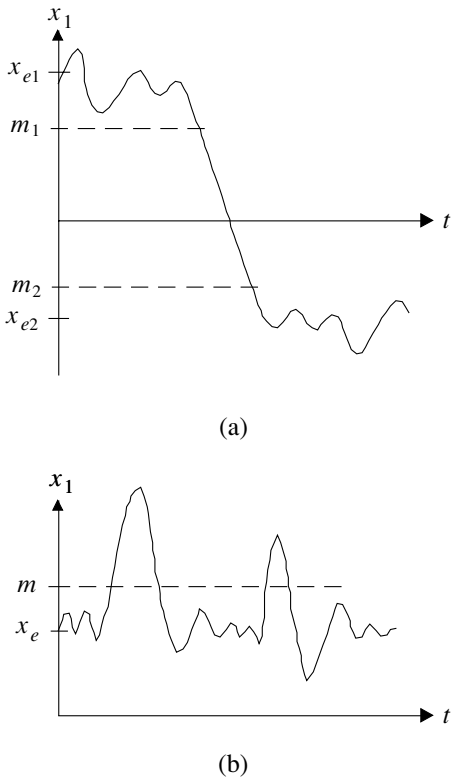

Fig. 2: Locating the dividing points by measuring amplitudes. (a) Excursion orbit traverses between neighborhoods of two saddle foci; (b) excursion orbit returns to neighborhood of the same saddle focus.

system. The system of equations can be written as v_{S1}, v_{S2} and i_{S3} for the drive system, and v_{R1}, v_{R2} and i_{R3} for the response system. The system of equations can be written as

$$\begin{aligned}
\dot{v}_{S1} &= \left(\tfrac{v_{S2}-v_{S1}}{R} - f(v_{S1})\right)/C_1 \\
\dot{v}_{S2} &= \left(\tfrac{v_{S1}-v_{S2}}{R} + i_{S3}\right)/C_2 \\
\dot{i}_{S3} &= -v_{S2}/L \\
\dot{v}_{R1} &= \left(\tfrac{v_{R2}-v_{R1}}{R} - f(v_{R1})\right)/C_1 - k_1 k_{b1}(v_{R1} - v_{S1}) \\
\dot{v}_{R2} &= \left(\tfrac{v_{R1}-v_{R2}}{R} + i_{R3}\right)/C_2 - k_2 k_{b2}(v_{R2} - v_{S2}) \\
\dot{i}_{R3} &= -v_{R2}/L - k_3 k_{b3}(i_{R3} - i_{S3})
\end{aligned} \tag{17}$$

where subscripts S and R denote drive and response system variables respectively, k_1, k_2 and k_3 are the coupling gains corresponding to the three variables, and k_{b1}, k_{b2} and k_{b3} take either 1 or 0 according to whether the drive signals are sent or not sent. The function $f(.)$ that defines the nonlinear conductance is

$$f(v) = G_b v + \frac{1}{2}(G_a - G_b)(|v+E| - |v-E|) \tag{18}$$

where $G_a = -0.753$ mS, $G_b = -0.3965$ mS and $E = 1$ V.

Two sets of simulation are performed, corresponding to the following two coupling arrangements:

1. All three drive variables are simultaneously transmitted during the excursion intervals. In this case, $k_{b1} = k_{b2} = k_{b3} = k_b$, and k_b is as defined in (10).

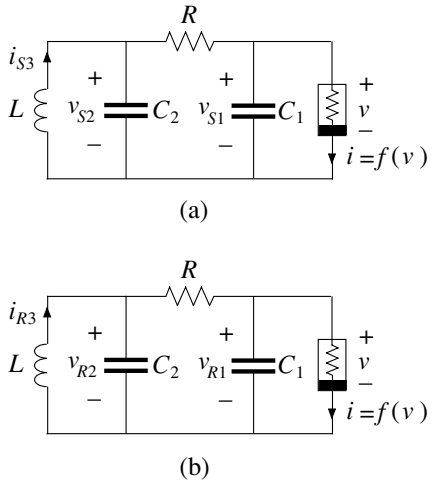

Fig. 3: Chua's circuits. (a) Drive system, (b) response system.

2. The three drive variables are transmitted successively one at a time during the excursion intervals. In this case, k_{b1}, k_{b2} and k_{b3} are given by (12) to (14). Note here that only one signal has to be transmitted in practice.

In both cases, the excursion intervals are determined using the amplitude measurement method discussed in Section 3. The circuit parameters are: $C_1 = 10$ nF, $C_2 = 100$ nF, $L = 18$ mH and $R = 1.68$ kΩ. The initial conditions are set at $(v_{S1}, v_{S2}, i_{S3}) = (0.8, -0.3, 0.0)$ and $(v_{R1}, v_{R2}, i_{R3}) = (0.3, 0.7, 0.0)$. Results are shown in Figs. 4 (a) to (c) for the case of simultaneous coupling, and in Figs. 4 (d) to (f) for the case of successive coupling. In both cases, we verify that synchronization can be achieved using this non-continuous excursion-orbit coupling approach.

5. Conclusion

This paper describes a novel approach for chaos synchronization, in which the drive signals are transmitted only for very short intervals of time, leading to large saving in transmission bandwidth. The method is based on the viewpoint that the chaotic orbit is composed of a "spiraling" orbit and an "excursion" orbit, and the attractor is strongly characterized by the "excursion" orbit. Thus, synchronization can be achieved by coupling only the 'excursion" orbit.

References

[1] L.M. Pecora and T.L. Carroll, "Synchronization in chaotic systems," *Phys. Rev. Lett.,* **64**, 821–824, 1990.

[2] L. Kocarev, K.S. Halle, K. Eckert, L.O. Chua and U. Parlitz, "Experimental demonstration of secure communications via chaotic synchronization," *Int. J. Bifur. Chaos,* **2**(3), 709–713, 1992.

[3] K.S. Halle, C.W. Wu, M. Itoh and L.O. Chua, "Spread spectrum communication through modulation of chaos," *Int. J. Bifur. Chaos,* **3**(2), 469–477, 1993.

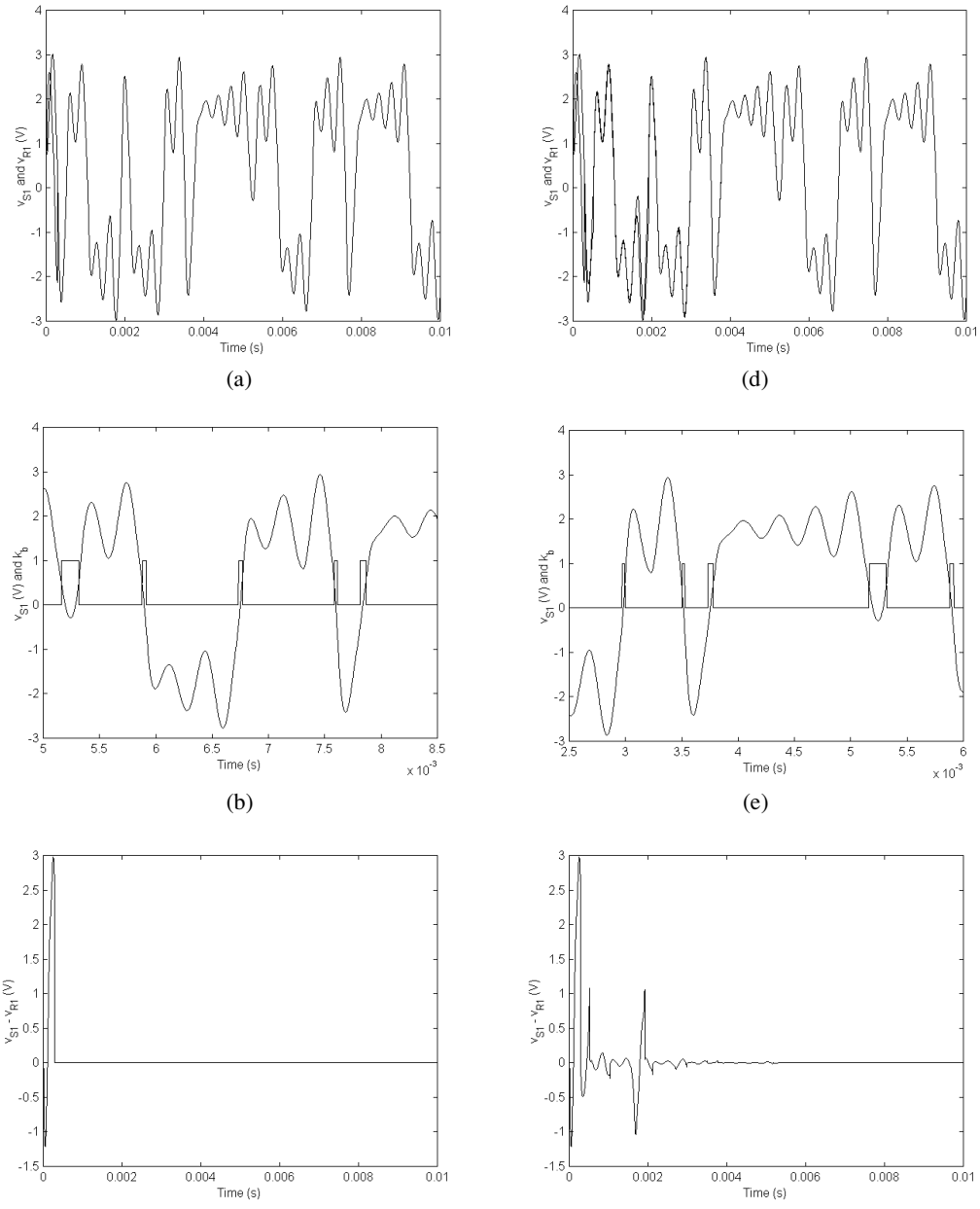

Fig. 4: Left column: synchronization of Chua's circuits with simultaneous transmission of all drive variables. $k_x = k_y = k_z = 0.7$. (a) v_{S1} and v_{R1}, (b) v_{S1} and k_b showing the coupling intervals, (c) synchronization error $v_{S1} - v_{R1}$; Right column: synchronization of Chua's circuits with successive (one-at-a-time) transmission of all drive variables. $k_x = k_y = k_z = 0.7$. (d) v_{S1} and v_{R1}, (e) v_{S1} and k_b showing the coupling intervals, (f) synchronization error $v_{S1} - v_{R1}$.

[4] C.W. Wu and L.O. Chua, "A simple way to synchronize chaotic systems with applications to secure communication systems," *Int. J. Bifur. Chaos,* **3**(6), 1619–1627, 1993.

[5] I. Procaccia, "Universalities of dynamically complex systems: the organization of chaos," *Nature,* **333**, 618–623, 1988.

[6] S.S. Qiu, "Refined and extension description of the cell model of chaotic attractors (I)," *J. South China Univ. Tech. (Natural Sci. Ed.),* **28**(12), 18–23, 2000.

[7] L.P. Shil'nikov, "A case of the existence of denumerable set of periodic motions," *Sov. Math. Dokl.,* **6**, 163–166, 1965.

[8] L.P. Shil'nikov, "Chua's circuit: rigorous results and future problems," *Int. J. Bifurc. Chaos,* **4**, 489–519, 1994.

[9] K. Pyrages, "Continuous control of chaos by selfsynchronizing feedback," *Phys. Lett.,* **A170**(6), 421–428, 1992.

[10] R.N. Madan (ed.) *Chua's Circuit,* World-Scientific, 1993.